ESTIMATION OF ALUMINUM AND ARGON ACTIVATION SOURCES IN THE HANARO COOLANT

BYUNG JIN JUN*, BYUNGCHUL LEE and MYONG-SEOP KIM
Korea Atomic Energy Research Institute
1045 Daedukdaero, Yuseong-gu, Daejeon, 305-353, Korea
*Corresponding author. E-mail : bjjun@kaeri.re.kr

Received November 16, 2009
Accepted for Publication May 06, 2010

The activation products of aluminum and argon are key radionuclides for operational and environmental radiological safety during the normal operation of open-tank-in-pool type research reactors using aluminum-clad fuels. Their activities measured in the primary coolant and pool surface water of HANARO have been consistent. We estimated their sources from the measured activities and then compared these values with their production rates obtained by a core calculation. For each aluminum activation product, an equivalent aluminum thickness (EAT) in which its production rate is identical to its release rate into the coolant is determined. For the argon activation calculation, the saturated argon concentration in the water at the temperature of the pool surface is assumed. The EATs are 5680, 266 and 1.2 nm, respectively, for Na-24, Mg-27 and Al-28, which are much larger than the flight lengths of the respective recoil nuclides. These values coincide with the water solubility levels and with the half-lives. The EAT for Na-24 is similar to the average oxide layer thickness (OLT) of fuel cladding as well; hence, the majority of them in the oxide layer may be released to the coolant. However, while the average OLT clearly increases with the fuel burn-up during an operation cycle, its effect on the pool-top radiation is not distinguishable. The source of Ar-41 is in good agreement with the calculated reaction rate of Ar-40 dissolved in the coolant.

KEYWORDS : HANARO, Pool Type Research Reactor, Aluminum-clad Fuel, Coolant Activity Source, Oxide Layer, Na-24, Ar-41

1. INTRODUCTION

Aluminum-clad fuels are commonly used in high-power research reactors. Three major radioactive nuclides, Na-24 ($t_{1/2}$ 15.0 h), Mg-27 ($t_{1/2}$ 9.46 m), and Al-28 ($t_{1/2}$ 2.31 m), are produced by neutron activation of Al-27 in the reactor with the aluminum-clad fuels from $(n,\alpha)^{24}Na$, $(n,p)^{27}Mg$, and $(n,\gamma)^{28}Al$ reactions, respectively. Some of the nuclides are released into the coolant, becoming the major radiation sources in the primary cooling system next to N-16 ($t_{1/2}$ 7.13 s), produced by $^{16}O(n,p)^{16}N$. If the reactor has an N-16 decay tank and if other strong sources do not exist, the aluminum activation products govern the radiation after the decay tank. In an open-tank-in-pool type reactor, they also govern the activity of the pool water and radiation at the pool top, where personnel as well as visitors may frequently approach. Therefore, to determine the volume of the decay tank and a shield for the primary cooling system and ion exchangers and to predict the pool-top radiation level during normal operation, an estimation of the sources of aluminum activation products is necessary.

Ar-41 ($t_{1/2}$ 1.83 h) is produced via the $^{40}Ar(n,\gamma)^{41}Ar$ reaction of which the residue is finally released into the environment. This represents one of the major radionuclides released into the environment during the normal operation of a research reactor. Its source from the pool can be predicted by estimating the saturated argon concentration in the coolant.

In HANARO, a 30 MW open-tank-in-pool type research reactor with aluminum-clad fuels, a quantitative analysis of the radionuclides in the primary coolant sample by gamma-ray spectroscopy is conducted periodically to monitor any abnormal release of radionuclides into the coolant. The pool surface water is occasionally analyzed by the same method. In samples of the primary coolant, the activities of aluminum activation products are the majority, with the second most important being Ar-41 followed by the fission products and W-187. At the pool surface, short half-life nuclides, including Mg-27 and Al-28, are below the detection limit due to the sufficient float up delay; hence, Na-24 becomes the majority with minor Ar-41, Xe-133 and a few other fission products. While the relative standard deviations of other nuclides are large, those of aluminum activation products and Ar-41 are reasonable for the estimation of their sources.

We estimated the sources of the aluminum activation

products and Ar-41 in the coolant from the measured activities using a lumped parameter model. The average production rate for each nuclide was calculated by MCNP5 [1]. The aluminum activation products are released into the coolant from the surface of the fuel clad; therefore, their EATs are determined from the sources, calculated production rates and fuel surface area. The production rate of each nuclide in its EAT is identical to its release rate into the coolant. If such equivalent thicknesses for materials in the core are available for respective activation products, it becomes possible to estimate their release rates into the coolant. However, the authors could not find relevant information regarding the core materials of HANARO that contain aluminum. Therefore, we also discuss possible explanations for the obtained EATs. For Ar-41, its source is compared with its total production rate in the coolant when the argon concentration in the coolant is saturated at the pool surface temperature.

2. SOURCE ESTIMATION MODEL

A conceptual diagram of the primary cooling system and the reactor pool of HANARO is shown in Fig. 1. The numbers at the left side of the pool represent the pool depth in meters at their respective elevations. In order to suppress pool-top radiation, a hot water layer is formed at the upper part of the pool by the heaters of a hot water layer system. From the measured vertical distributions of the pool water temperature and the Na-24 activity [2], it was confirmed that the reactor pool of HANARO could be divided into three layers according to a nearly stepwise temperature

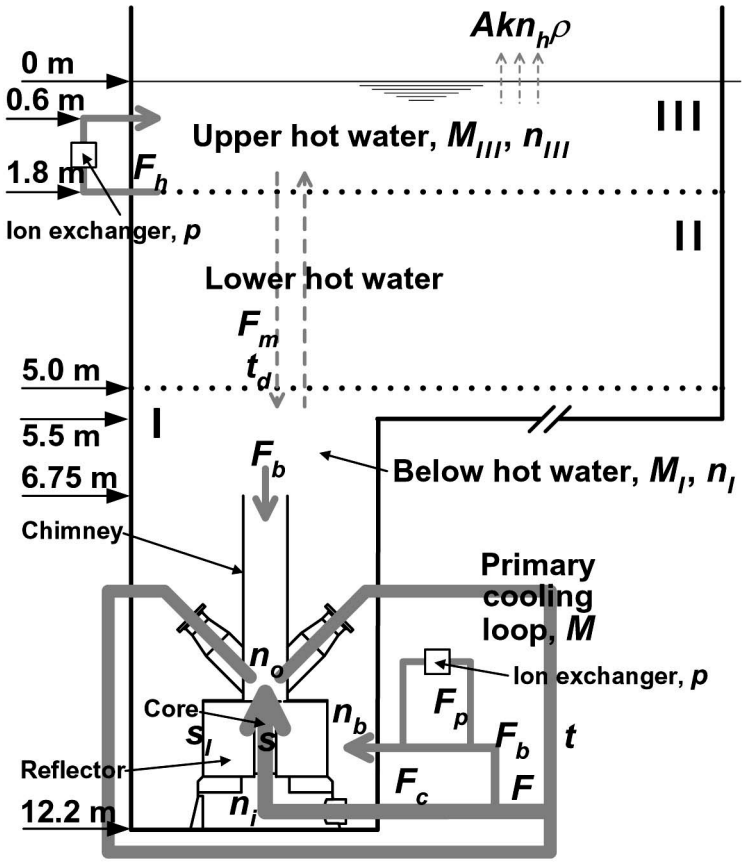

Fig. 1. Primary Cooling Loop and Pool Model

distribution; these were a pool region below the hot water layer (Region-I), a lower hot water layer (Region-II) and an upper hot water layer (Region-III). Boundaries were set at depths of 1.8 and 5 m. The Na-24 activity in Region-I was almost constant regardless of the depth; it decreased sharply in Region-II and was then almost constant again in Region-III. Therefore, we divided the pool into three regions in addition to the primary cooling region for analysis by a lumped parameter model.

The overall concept of the model is depicted in Fig. 1 as well. In this model, the coolant flow rate is the mass flow rate and the nuclide concentration is the nuclide number density per coolant mass. The primary coolant, of which the total flow rate and circulation time are F and t, respectively, splits into a core flow F_c and a bypass flow F_b before its entry into the core. Some of the bypass flow passes through a primary coolant purification system at a flow rate of F_p, and an ion exchanger cleans up ionized nuclides in the water with efficiency p, i.e., the nuclide concentration after the ion exchanger is reduced to a portion of (1 - p). The bypass flow, having a nuclide concentration of n_b, is then discharged into the pool. A primary coolant sampling tube is connected to the entrance to the ion exchanger. The coolant reaches this location nearly in unison with its arrival at the core. Therefore, it is assumed that the measured activity represents the core inlet activity. As the bypass flow goes to the pool quickly, its decay to discharge is neglected. The nuclide concentration n_i at the core inlet increases to n_o, the concentration at the core exit, due to the source term s in the core. As the coolant passes through the core in about 0.1 seconds, radionuclide decay in the core is neglected but the time required for the coolant to pass through the core is included in the primary coolant circulation time t. At the core outlet, the core flow meets the bypass flow coming down from Region-I having an average nuclide concentration of n_I through the chimney. The down flow at the chimney prohibits the floating up of the core flow to the pool surface. At a steady state, Eq. (1) represents the balance for a nuclide in the primary cooling loop.

$$Fn_i = (F_c n_i + s + F_b n_I)e^{-\lambda t} \tag{1}$$

In Region-I with water mass M_I, the nuclide is produced by source s_I in the pool and comes in from the primary cooling system through the bypass flow and from Region-III through Region-II by mixing flow F_m. Meanwhile, it decays out with decay constant λ, goes back into the primary cooling system through the chimney, and escapes to Region-III through Region-II. This can be expressed as shown below:

$$F_b n_b + s_I + F_m n_{III} e^{-\lambda t_d} = (M_I \lambda + F_b + F_m) n_I \tag{2}$$

Here, n_{III} is the nuclide concentration in Region-III and t_d is the time required to pass through Region-II by the mixing flow.

In Region-II, F_m and t_d above are hypothesized. As the transport phenomenon in this layer is a key to determining the pool-top radiation, an understanding of this is required to determine an effective means of suppressing the pool-top radiation, for which a study has not yet been undertaken. In this study, the hypothesis above is chosen because a preliminary study of the variation of pool-top radiation based on it showed good agreement with the actual trend for an initial rise of pool-top radiation at the beginning of the reactor operation.

In Region-III with water mass M_{III}, ionized nuclides are cleaned up by an ion exchanger of the hot water layer system with a flow rate of F_h. Its cleanup efficiency is assumed to be identical to that of the primary cooling purification system. At the pool surface, volatile gases are exchanged with air and are then released into the environment through the filters of a reactor ventilation system. The loss rate of a volatile nuclide from the hot water layer to the air is a product of the pool surface area A, the gas exchange coefficient k, the nuclide number density n_{III} per unit water mass, and the water density ρ. While some water moves down to Region-I, its counter flow carries nuclides from Region-I by mixing flow F_m.

Among the above parameters, all flow rates except F_m are known, the nuclide concentrations at the core inlet and the hot water layer are measured, and the cleanup efficiency in the ion exchangers and the loss coefficients of volatile nuclides to the air can be measured. If a nuclide is also produced in the pool by s_I, its ratio to s can be estimated from the reaction rates in the core calculation. Subsequently, from the steady state balance equations for each nuclide, the source term s in the core and the value of F_m can be determined.

The measured data show that n_{III} must be less than 1% of n_I, which also indicates that F_m must be much smaller than F_b. Therefore, the term coming in from Region-III in Eq. (2) is neglected. When $F_b n_b$ is replaced by $F_b n_i$-$pF_p n_i$, Eqs. (1) and (2) give s by

$$s = \frac{C_1 n_i}{1 + \gamma C_0}, \tag{3}$$

where γ is the pool source ratio. It is defined as

$$\gamma = \frac{s_I}{s},$$

$$C_0 = \frac{F_b}{\lambda M_I + F_b + F_m}, \text{ and}$$

$$C_1 = Fe^{\lambda t} - F_c - C_0(F_b - pF_p).$$

To make the calculated n_{III} values for Na-24 and Ar-41 agree with measured ones, F_m must be less than 1% of F_b. Therefore, F_m in C_o can also be neglected. Thus, s is determined to be independent of any parameters in the hot water layers.

3. ESTIMATION OF SOURCES

3.1 Data for source estimation

During the normal operation of HANARO, the species and concentrations of the radionuclides in the primary coolant except for the very short-lived nuclides were determined using the gamma-ray spectroscopy. The primary coolant samples at the inlet and outlet of the primary coolant purification system were collected to measure the nuclide concentration and the cleanup efficiency of the ion exchanger. The volume of the collected water for each measurement was 100 cm^3, and the cooling time was 5 minutes. The coolant in the sampling line is sufficiently drained before sampling to eliminate stagnant water in the line. The full-energy peak efficiency for the volume source was calibrated using a cylindrical bottle-type standard source. For the density of the coolant sample, 1 g/cm^3 was used.

Given that the coolant flow time from the core outlet to the sampling point is similar to the time to the core inlet, it is assumed that the measured activity at the ion exchanger inlet represents the core inlet activity as well. The cleanup efficiency p of the ion exchanger is determined from the ratio of activities at the outlet and inlet of the ion exchanger. The pool water mass M_I is calculated for a water volume below 5 m depth, but structures in the pool, including the core and the reflector, are neglected. The pool source ratio γ is estimated by a core calculation using MCNP5 in which nearly the actual core geometry is modeled. The reactor design and operation data are used for other parameters.

The average values of the activity measurements of the nuclides of interest in the coolant and their standard deviations are represented in Table 1. The standard deviation for Al-28 is much larger than those of other nuclides due to its short half-life.

To determine the cleanup efficiency p of the ion exchanger, the activities at the ion exchanger outlet were also measured five times during the first quarter of 2009. The first measurement was when the ion exchanger was near the end of its life and the other four were after it was replenished with fresh resin. The cleanup efficiency was 0.845 for both Na-24 and Mg-27 at the first measurement and 0.899 ~ 0.975 after the resin was replaced. No noticeable difference between Na-24 and Mg-27 was found. Because one gamma-ray spectroscopy system was used, an efficiency measurement for Al-28 was not possible due to its short

Table 1. Measured Activities of the Radionuclides of Interest in the Primary Coolant, Estimated Sources and Equivalent Aluminum Thicknesses

Nuclide	Na-24	Mg-27	Al-28	Ar-41
Average activity* (Bq/cm^3)	1.52×10^3	5.50×10^3	1.59×10^3	3.67×10^2
Standard deviation of the activity* (%)	14.6	15.3	65.8	12.1
Source (/s)	9.8×10^{11}	2.6×10^{11}	4.3×10^{10}	3.4×10^{10}
Equivalent Al thickness (nm)	5680	266	1.2	**

* For 28 measurements in 2006 and 2007

** The calculated $^{40}Ar(n,\gamma)\ ^{41}Ar$ reaction rate in the primary coolant for the saturated argon concentration at 45 ˚C is 3.3×10^{10} /s.

half-life. The activity of Ar-41 at the ion exchanger outlet was nearly identical to that of the inlet. The coolant conductivities at the inlet and outlet of the ion exchanger were nearly steady while the ion exchanger worked normally; they increased rather rapidly when the resin reached the end of its service life. There is no available p value for Al-28, but its contribution to the result is practically negligible, as discussed in section 3.4. Therefore, we assume that the cleanup efficiency p is approximately 0.9 for Na-24, Mg-27 and Al-28 during the entire life cycle of the resin. However, this value is 0 for Ar-41.

The pool source ratio γ was calculated only for Ar-41 because the majority of aluminum activation products come from the fuel surface. The calculated value of γ for Ar-41 is 0.13.

3.2 Estimated sources

Estimated sources using the above factors and Eq. (3) are shown in Table 1. In addition to source estimation using the measured activity, for the case of Ar-41, its source was also estimated by a core calculation for the radiative capture reaction of the dissolved argon gas. In this calculation, the saturated Ar-40 concentration in the coolant is deduced from the solubility of the argon gas in the water in a normal atmospheric environment, as suggested by Hamme and Emerson [3]. While the usual pool surface temperature of HANARO is about 45 ˚C, their correlation for solubility is valid within the range of 1 ~ 30 ˚C. However, their values up to 60 ˚C divided by the argon volume fraction of 0.9342% in air are close to the data openly available on the Internet [4]. A solubility of 3.6935×10^{-4} g-Ar/kg-water at 45 ˚C was used. The calculated source for Ar-41 is given in the notes attached to Table 1. It is very close to the value estimated from the measured activity in the primary coolant.

3.3 Uncertainty of estimated sources

Uncertainty of the estimated sources consists of the statistical uncertainty of the measured primary coolant activities, assumptions in the lumped parameter model and the uncertainty of the parameters used in the model. Among them, the standard deviations of the measured primary coolant activities are listed in Table 1.

Eq. (1) takes into account the decay of the nuclide while the coolant circulates the primary cooling loop. Therefore, the model deals with the actual phenomenon almost exactly. In Region-I, however, Eq. (2) assumes that the bypass flow coming to the pool is immediately mixed with the pool water and that the pool water activities become immediately homogeneous. However, there would be a flow path in the pool from the pool inlet of the bypass flow to the pool outlet at the chimney. Then, the averaged maximum decay time t_{max} in the pool can be M_I/F_b, which is deduced to 35.2 minutes. In this case, the concentration of a nuclide in the water coming down from the chimney and being mixed with the core exit flow is

$$n_I^1 = n_b e^{-\lambda t_{\max}} \tag{4}$$

instead of n_I. The relationship between the source s and core inlet concentration n_i then becomes Eq. (5),

$$s = \frac{C_{11} n_i}{1 + \gamma C_{01}}, \tag{5}$$

where,

$$C_{01} = e^{-\lambda t_{\max}} \text{ and}$$

$$C_{11} = F e^{\lambda t} - F_c - C_{01}(F_b - p F_p).$$

In the equations above, it is assumed that a nuclide produced in the pool by the pool source s_I decays for t_{max} as well before being mixed with the core exit flow. The sources estimated by Eq. (5) are 0, 15, 2.8 and 8.1% larger than those by Eq. (3) for Na-24, Mg-27, Al-28 and Ar-41, respectively. Considering that the calculated value of t_{max} is much shorter than the half-life of Na-24, there is almost no difference in Na-24. In the case of Al-28, because the contribution of the bypass flow coming down from the chimney is very small in the core outlet activity, its difference is small compared to Mg-27 and Ar-41.

Among the parameters used in the model, the uncertainties in the pool water mass M_I and ion exchanger cleanup efficiency p are larger than others. The major uncertainty in M_I comes from neglecting the structures in the pool. As shown in Fig. 2, only Ar-41 is rather sensitive to M_I, as its decay in the pool is a major loss term and because there is no loss by cleanup. The sensitivities are 0.13, 0.15, 0.026 and 0.7 %/%-M_I for Na-24, Mg-27, Al-28 and Ar-41, respectively.

Sensitivities to cleanup efficiency p are shown in Fig. 3. Only Na-24 is sensitive owing to its rather long half-life. Cleanup is about 83% in the total loss of Na-24, which is about 5 times its total decay. These sensitivities are 0.9, 0.037 and 0.005 %/%-p for Na-24, Mg-27 and Al-28, respectively.

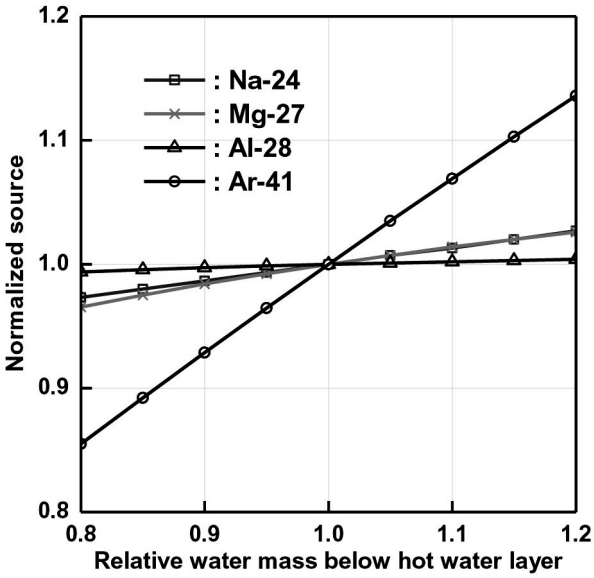

Fig. 2. Sensitivity of Sources on the Pool Water Mass Below the Hot Water Layer

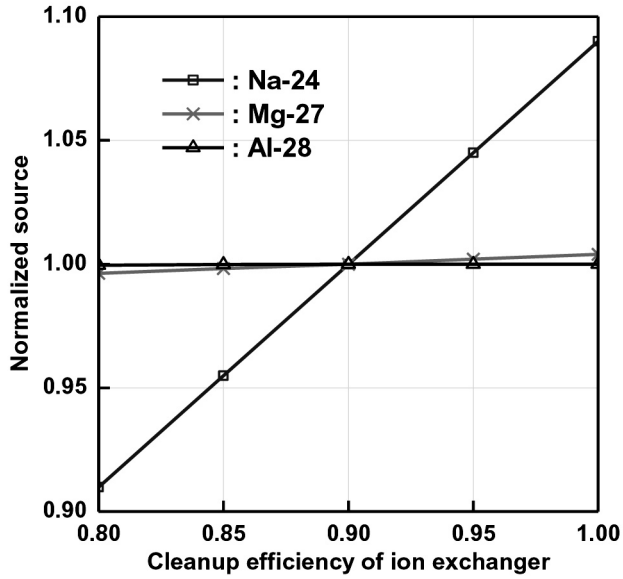

Fig. 3. Sensitivity of Sources on the Ion Exchanger Cleanup Efficiency

The above results from the sensitivity study can be summarized as follows:

The Na-24 source is sensitive only to the ion exchanger cleanup efficiency *p*. The *p* value is usually larger than 0.9 while the resin maintains its performance level, though it rapidly decreases to about 0.845 at near end of its life, as explained in section 3.1. Therefore, we can safely assume that the bias of *p* from 0.9 is well within 5%. Thus, the reliability on the Na-24 source given in Table 1 is within 5% bias with a standard deviation of 14.6%.

The lumped parameter model causes the largest uncertainty for the Mg-27 source. The Mg-27 source can be up to 15% larger value than that in Table 1 with standard deviation slightly larger than 15.3%. There is no considerable additional uncertainty for the Al-28 source. The majority of its uncertainty comes from its activity measurement, of which the standard deviation is 65.8%.

For the Ar-41 source, the lumped parameter model underestimates the source by a maximum of 8.1%. Its sensitivity to M_l is 0.7 %/%-M_l. If structures in the pool are considered, the actual value of M_l is nearly 10% smaller and the source becomes about 7% smaller. As these two uncertainties offset each other, uncertainty of 8% can be conservatively assumed. In addition, the calculated sensitivity to the pool source ratio γ is 0.72 %/%-γ. If the uncertainty in the calculation of Ar-41 in the core and in the pool is assumed to be 20%, the uncertainty regarding the estimation of γ is about 30%. Given that the calculated value of γ is approximately 0.13, its uncertainty is about 0.04, which results in nearly 3% uncertainty of the source. When the standard deviation of 12.1% in the Table 1 is added, the combined uncertainty for Ar-41 source is about 15%.

3.4 Equivalent aluminum thickness

The production rates of the aluminum activation products are calculated by the core calculation. The EAT for each product is therefore obtained by dividing its source by the total aluminum surface area and its reaction rate per unit volume of aluminum. The deduced EATs are presented in Table 1.

Na-24 and Mg-27 are produced by fast neutrons with threshold energies at 3.25 MeV and 2.5 MeV, respectively. The Na-24 and Mg-27 nuclides produced in the aluminum recoil with energies according to the Q-values of the reactions. However, their flight lengths in the aluminum are much smaller than their EATs shown in Table 1. Similarly, the release of Al-28 to the coolant by recoil cannot feasibly explain its EAT value. Less than 1% of Al-28 is produced by the fast neutron reactions. Therefore, should the Al-28 be released into the coolant only by recoil from the fast neutron reactions, the EAT for Al-28 produced by fast neutrons would be larger than 100 nm, which is much larger than the flight length of the recoiled Al-28. The thermal neutron capture also recoils the compound nucleus by the emission of prompt gamma ray(s). However, it is quite doubtful whether the recoil can result in the EAT value.

The EAT of 5.68 μm for Na-24 is similar to the average

OLT at the cladding surface of HANARO fuel. Chae et al. [5] measured the OLT according to the burn-up for HANARO fuel and made the following correlation:

$$X_{ox} = 0.0049B^{2.1063} \quad (6)$$

Here, X_{ox} is the OLT in μm and B is the burn-up in atomic percent of U-235. The estimation of average OLTs in the core using above equation is as follows:

The HANARO core has 32 fuel assemblies composed of eight batches. As the average discharge burn-up of U-235 is about 55%, the core-averaged burn-up increases by 6.875% during a cycle. Assuming that all fuel assemblies burn uniformly, the difference in the average burn-up between two adjacent batches is 6.875 %. Hence, the batch average burn-ups range from 0 to 48.125 % at the beginning of the cycle (BOC) and from 6.875 to 55 % at the end of the cycle (EOC). The average OLTs at BOC and EOC are calculated using Eq. (6) assuming that the burn-up distribution is uniform within the above ranges, resulting in 5.5 μm at the BOC and 8.3 μm at the EOC. The atomic number density of the aluminum in the aluminum metal is similar to that in Al_2O_3 single crystal, which has theoretical density. However, the actual density of the oxide layer appears to be considerably lower than the theoretical density of Al_2O_3. Thus, the areal density of the aluminum atoms in the EAT deduced for the Na-24 nuclide is close to that in the OLT estimated for the EOC. Though it is a rough estimation, the opinion that the EAT for Na-24 is similar to the average OLT appears to be tenable.

Kim et al. [6] stated, "The oxide layer has numerous thin cracks and consists of a protective oxide (Al_2O_3) and hydrated oxides ($Al_2O_3 \cdot H_2O$ and $Al_2O_3 \cdot 3H_2O$). These oxide-hydrates are soluble in water, especially in flowing water." They did not explore the kinetics of cladding wall thinning nor did they assess oxide dissolution, but we surmise that the activated products are released into the coolant due to their dissolution in the oxide layer.

The sequence of the EATs deduced for the nuclides of interest coincides with the sequences in the solubility in water and with the half-life. The actual release would not be limited to the EAT but may stem from entire oxide layer. However, the nuclides with lower solubility and shorter half-life dissolve less and decay more until they escape the oxide matrix. Meanwhile, it is clear that the dissolution rate of Al-28 is much greater than the dissolution rate of the oxide-hydrates. If the decay of the Al-28 before escaping the oxide layer is taken into account, the actual dissolution of Al-28 should be more than this estimation. If the dissolution of Al-28 results from the dissolution of the oxide-hydrates, the cladding thickness is reduced by more than 1.2 nm per second. Hence, the cladding would disappear very rapidly. This was not observed. It appears that some Al-28 nuclides in the oxide layer are ionized due to the neutron capture mechanism and are dissolved into the coolant much more readily than the oxide-hydrates.

Given that the average OLT increases by nearly 50 % during an operation cycle, an increase of the aluminum activation products in the coolant with the reactor operation time during an operation cycle is expected. However, the pool-top radiation governed by Na-24 is usually almost constant after it is saturated.

4. CONCLUSION

The sources of aluminum and argon activation products in the coolant of HANARO are estimated from their activities measured in the primary coolant and the lumped parameter model simulating the balance of each product in the primary cooling loop and in the pool. The statistical uncertainty of the measured activities is confirmed as the largest portion in the uncertainty of the estimated sources. The estimated Ar-41 source is in good agreement with the calculated argon activation for the saturated argon concentration in the water at the temperature of the pool surface. The EATs of the aluminum activation products coincide with their solubility values in the water and their half-lives. The EAT of Na-24 is similar to the average OLT of the fuel cladding, which indicates that almost all of the Na-24 in the oxide layer is released into the coolant. It can be considered that Mg-27 and Al-28 are also released into the coolant from the entire oxide layer, but their EATs are much smaller than the average OLT due to their low solubility levels and short half-lives. The average OLT noticeably increases with the fuel burn-up during an operation cycle. Therefore, it is expected that the sources of aluminum activation products gradually increase during the cycle. However, the pool-top radiation is usually almost constant after saturation. Should similar analyses be applied to many other research reactors using aluminum-clad fuels, a reliable database could be produced.

ACKNOWLEDGEMENT

The study was conducted under a MEST (Ministry of Education, Science and Technology) project of the Korean Government for research reactor technology. Careful measurements of the coolant radioactivity by the HANARO operation group and the valuable discussions with Dr. J.H. Park, H.T. Chae and J.M. Park regarding the flow mechanism in the pool and the oxide layer of the fuel are highly appreciated.

REFERENCES

[1] T. E. Booth, et al., "MCNP – A General Monte Carlo N-Particle Transport Code", **Version 5**, LA-UR-03-1987, Los

Alamos National Laboratory (2005).
[2] K. H. Ahn, et al., "Analysis on the variation of pool-top radiation in HANARO", KAERI/TR-1432/99, Korea Atomic Energy Research Institute (1999). [in Korean]
[3] R. C. Hamme and S. R. Emerson, "The solubility of neon, nitrogen and argon in distilled water and sea water", *Deep-Sea Research*, **I 51**, 1517 (2004).
[4] Solubility of gases in water, http://www.engineeringtoolbox.com/, visited on 31 March 2010.
[5] H. T. Chae, H. Kim, C. S. Lee, B. J. Jun, J. M. Park, C. K. Kim, and D. S. Sohn, "Irradiation tests for U3Si-Al dispersion fuels with aluminum cladding", *J. Nucl. Materials*, **373**, 9 (2008).
[6] Yeon Soo Kim, G. L. Hofman, A. B. Robinson, J. L. Snelgrove, and N. Hanan, "Oxidation of aluminum alloy cladding for research and test reactor fuel", *J. Nucl. Materials*, **378**, 220 (2008).